Optimal configuration of isolated hybrid AC/DC microgrids

Hamad, Amr A.; Nassar, Mohammed E.; El Saadany, Ehab F.; Salama, M. M. A.

Publisher's version / Version de l'éditeur:
https://doi.org/10.1109/TSG.2018.2810310
IEEE Transactions on Smart Grid, 2018-03-09

Optimal Configuration of Isolated Hybrid AC/DC Microgrids

Amr A. Hamad, Member, IEEE; Mohammed E. Nassar, Student Member,IEEE; Ehab F. El Saadany, Senior Member, IEEE; and M. M. A. Salama, Fellow, IEEE

Abstract— **This paper proposes a planning model for isolated microgrids according to which ac and dc zones are defined within a hybrid ac/dc paradigm. Furthermore, the size of the distributed generation and the energy storage systems are allocated for every zone as well as the capacity of the interlinking converters between zones with different types. The proposed formulation is a mixed integer nonlinear problem that minimizes the total investment and operational costs. Zone types, represented as integer variables in the problem, are critical factors that define the required energy converters and accordingly the overall investment cost and system losses. The operational criteria of each component within the microgrid are considered to provide reliable operational scenarios, and the active and reactive power adequacy of the microgrid is guaranteed since the presented formulation incorporates stochastic load and generation models. The validity and effectiveness of the introduced formulation are demonstrated through several case studies for different load topologies.**

Index Terms—**Distributed energy resources (DER), hybrid ac/dc microgrids, isolated microgrids, planning model.**

NOMENCLATURE

1. Acronyms

DER	Distributed energy resources
DG	Distributed generation
ESS	Energy storage system
SoC	State of Charge

2. Indices

ac	Subscript for the ac systems
B	Subscript for the ESS
ch	Superscript for the ESS charging mode
dc	Subscript for the dc systems
dis	Superscript for the ESS discharging mode
g	Index for distributed generation Resource (DG)
h	Index for hour
net	Subscript for the net power at the network end
t	Index of an interlinking converter
V	Subscript for the Capacitive units
z	Index for zone

3. Sets

F	Set of fuel-based DG units
L	Set of loads
T	Set of interlinking converters
W	Set of renewable DG units
η_z	Set of neighbouring zones of a zone (z)

4. Parameters

CC	Cost for load curtailment
CE	Levelized investment cost of an ESS maximum SoC
CF	Levelized energy cost of the fuel-based DG units
CI	Levelized investment cost of an inverter
CP	Levelized investment cost of a DG or ESS power
CR	Levelized investment cost of a rectifier
CT	Levelized investment cost of an interlinking converter
CV	Levelized investment cost of a capacitor
P_L^{max}	Maximum active load demand
$Q_{L_{ac}}^{max}$	Maximum reactive load demand
$S_{L_{ac}}^{max}$	Maximum apparent load demand
u_d	Day weight during the year
β	Fraction of the peak demand corresponding to a specific scenario
γ	Available active power ratio of a renewable DG
η	Efficiency of the ESS power cycle
ρ	Ratio of the system power losses
σ	Ratio of the system power security
Ω_d^{st}	Daily probability of a combined load-generation scenario
Ω_{gd}^{st}	Daily probability of a generation scenario
Ω_{ld}^{st}	Daily probability of a load scenario
Ω_{gdh}^{st}	Probability of a generation state at time segment h
Ω_{ldh}^{st}	Probability of a load state at time segment h
$\Omega_{gdh+1\|h}^{st}$ $\Omega_{ldh+1\|h}^{st}$	Generation and load probability of transition from a state at time segment h to another state at time segment h+1

5. Variable

IC	Total investment cost
M_z	Zone type (0 for dc, 1 for ac)

$\boldsymbol{P, Q}$	Active and reactive powers (+ve if produced)
P^{loss}	Associated power loss due to energy conversion
P^{Cap}	Maximum installed power of a DG, ESS and rectifier
Q^{cap}	The installed VAR of a capacitive unit
S^{cap}	Maximum apparent power of DG, inverter and interlinking converter
SoC^{Cap}	Maximum state of charge of an ESS
SoC^{min}	Minimum state of charge of an ESS
α	Load curtailment ratio

II. Introduction

The advent of electronically based distributed generation (DG) and the radical changes in the nature of loading have promoted power distribution in a dc paradigm. On one hand, greater economies could be achieved if renewable energy resources such as wind and photovoltaic (PV), and energy storage systems were integrated into dc rather than ac systems. On the other hand, major loads such as modern elevators operate based on variable speed drives [1]. Plug-in electric vehicles (PEVs) represent a crucial factor in future electric distribution systems, and extensive electronic loads do exist in all modern homes with new inventions, including high-quality and highly efficient dc lighting systems. Further considerations are the intuitive merits of dc systems: reduction of interference with AC grids and facilitation of expanded power capacity. Thus, the concept of dc systems is emerged for active distribution systems and isolated microgrids as well.

The concept of isolated Microgrids has recently attracted significant attention since it provides a viable solution for remote community electrification. Isolated microgrids can eliminate investments on additional generation and transmission facilities to supply remote loads. Initiated as ac networks, similar to the common distribution systems, the construction of isolated microgrids has dramatically evolved to include dc and hybrid ac/dc systems that could adapt high penetration of dc-based DGs and loads [2]. Recent publications have addressed several operational and planning issues in isolated microgrids. Operational studies include modeling, energy management, load flow and stability have been extensively performed for the different isolated microgrid structures [3], [4]. However, the planning studies are performed mostly for ac microgrids. In [5], a probabilistic VAR planning was proposed. The presented formulation incorporates a high penetration level of intermittent energy resources to address the minimization of power loss within active and reactive power adequate profiles. In [6], Jun, et al. provide a coordinated sizing scheme for diesel generators and energy storage units to maintain the power adequacy in isolated microgrids. Based on the bifurcation theory, Guzmán et al. [7] introduced a scheduling methodology for the droop coefficients that improves the system frequency and voltage regulation. Morad, et al. [8] optimized the droop settings in isolated microgrids of the DGs to compromise the system loadability and the economical behavior according to the fuzzy utility function. The aforementioned work was extended in [9] to include the improvement in the system voltage profile as well.

To the best of the authors' knowledge, the configuration of isolated hybrid ac/dc microgrids has not been addressed yet in the literature. Therefore, in this work, an efficient planning model is proposed for these evolving networks. The objective of the formulation is to minimize the total planning cost, i.e., the investment cost of the DER mix and the associated electronic converters and the operational cost of the resultant interconnected microgrids. Due to the absence of a stiff subgrid and the high deployment of renewable DER, combined renewable-load stochastic scenarios are introduced to capture their intermit nature in the planning model. In addition, the detailed operational philosophy and power loss of each component are considered to present actual daily power schemes. The outcome of this formulation not only defines the boundaries of the ac and dc zones, but assigns the capacity of each DER in the zones as well as the capacity of the interlinking converters between the different type zones to achieve supply adequacy.

The remainder of the paper is organized as follows. Section III provides a brief overview of the presented problem. The modeling approach for the load and renewable DER is provided in section IV. Section V demonstrates the detailed planning formulation for the hybrid ac/dc microgrids. Section VI describes the numerical analysis and section VII concludes the paper.

III. Statement of the Problem

The rationale behind the work presented in this paper is to optimize the configuration of the isolated hybrid ac/dc microgrids with the consideration of comprehensive models for loading, generation, and electronic converters. In the planning model provided in [10], the active distribution system could be entirely constructed as an ac or dc network. The reactive component of the ac loads was not considered. In addition, renewable resources were neglected due to the existence of a main substation in the system. Similarly, the work proposed by the fourth author in this work [11] introduced a planning platform for system-connected hybrid ac/dc microgrids, and thus, the power adequacy was not of interest in the presented planning model .

In general, isolated microgrid structures can be divided into zones based on management, load profiles (such as residential, military, and industrial), and the majority of load type (ac or dc) [12], [13]. This work employs the latter approach to represent the microgrid as a set of mutually exclusive zones as illustrated in Fig. 1. The set of neighboring zones that can exchange power with zone z is denoted as $\mathcal{N}_z$, for instance, $\mathcal{N}_{z_2} = \{z_1, z_3\}$. With the absence of a main grid, this work provides a viable tool in defining the type of different zones (ac or dc) and the installed capacity of each DG type, the ESS, and the interlinking converters between the neighboring zones with different types. The proposed planning formulation aims at minimizing the total planning cost including the investment cost of the different DER resources as well as the operational cost. For simplicity purposes, other costs associated with distribution network upgrade and installation of additional

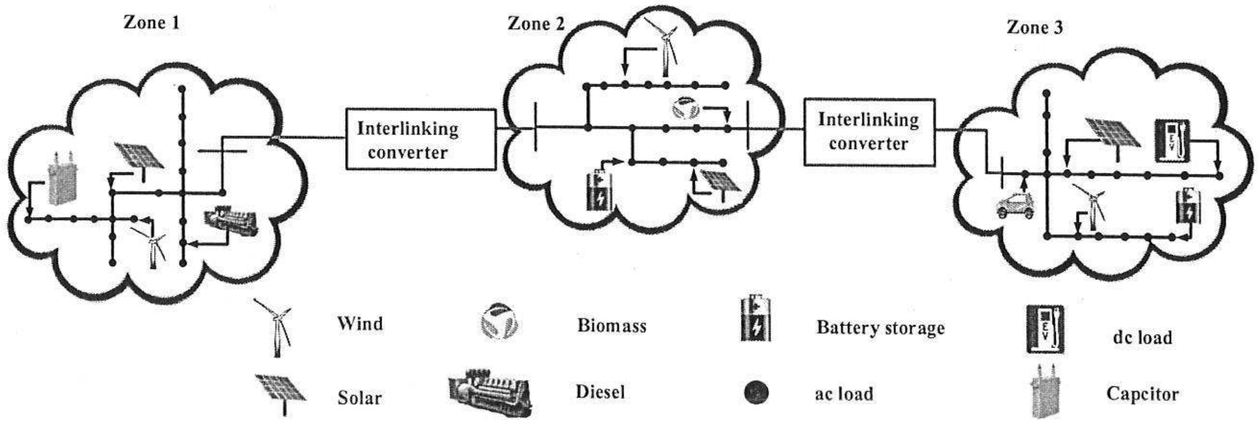

Fig. 1. Microgrid as mutually exclusive zones

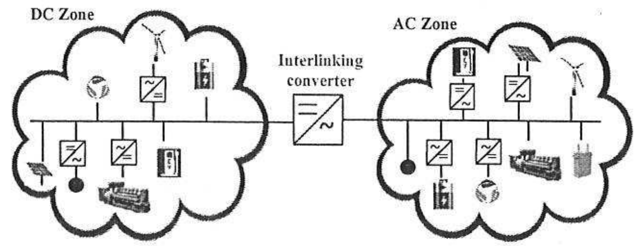

Fig. 2. Layout of a hybrid microgrid

transformers, switches, measurement devices, and controllers are ignored in this paper since these costs will be similar in both types of the microgrid [10].

In order to provide a reliable planning scheme, the intermittency nature of the load demand and renewable resources is considered via different stochastic scenarios as demonstrated in the following section. It is worth mentioning that planning of hybrid ac/dc systems is a sophisticated process. On one hand, the deployment of a specific DG type may incur additional power electronic conversion device and its associated power loss, according to zone type in which the DG is installed. Fig. 2 highlights the conversion stages to integrate DG units with ac vs dc systems. On the other hand, due to stochastic nature in the load and generation profiles, the adjacent zones may exchange their available active power. This power transfer would be throttled by the installed interlinking converter capacity, if the zones are defined with different types.

IV. Probabilistic DG and Load Modeling

A successful planning strategy for Microgrids should take into consideration the stochastic nature of both the renewable resources and loads. This section explains the analytical development of a combined generation-load scenarios that describe all possible system states and their respective probabilities. In general, the generation states model for variable power DG units is calculated by dividing the continuous probability distribution function (PDF) into several states. Considering the nonlinear relation between output power and wind speed, using wind speed states to model the probabilistic behavior of wind-based DGs becomes inadequate and may render the accuracy of the planning approach. Similarly, modeling the output power from solar-based DGs using irradiance states is insufficient. That is why the authors of this work developed a probabilistic model for the per unit output power obtained from wind and solar based DGs using PDF fitting and goodness-of-fit test [14]. Accordingly, the normalized and continuous PDF of the output power for each renewable source, instead of the wind speed or the solar irradiance, is divided into discrete states with the corresponding state probability calculated as follows:

$$\Omega_{renewable}^{st} = \int_{P_{st,min}}^{P_{st,max}} f(p)\, dp \qquad (1)$$

where $f(p)$ is the distribution probability of power and P_{min}^{st} and P_{max}^{st} are the minimum and maximum power limits of state "st," respectively.

The studies in [15] revealed no significant differences between the results obtained using this analytical approach and those obtained using Monte Carlo simulation (MCS).

The number of states for each component should be carefully selected so that the simplicity and accuracy of the analysis are not compromised: a large number of states increases accuracy but at the expense of also adding to the complexity, and a small number of states has the opposite effect. In this analysis, the year is represented by eight days, a weekday and a weekend for each season. At each of the presented 384 hours (2 days × 4 seasons× 24 hours), a probability $\Omega_{g,d,h}^{st}$ is defined for the states of intermittent generated power, based on the historical available data. In order to consider the correlation between the generated powers at successive time segments, a finite-state Markov model is utilized. Thus, the probability of a daily generation scenario could be calculated as

$$\Omega_{g,d}^{st} = \Omega_{g,d,1}^{st} \prod_{h=1}^{23} \Omega_{g,d,h+1|h}^{st} \qquad (2)$$

Similar approach is applied in order to obtain the probabilities of the daily load states as

$$\Omega_{l,d}^{st} = \Omega_{l,d,1}^{st} \prod_{h=1}^{23} \Omega_{l,d,h+1|h}^{st} \qquad (3)$$

Different loads and intermittent generation sources are uncorrelated; thus, the joint probability of a daily generation-load scenario Ω_{d}^{st} , describing a possible combination of generation and load states in the microgrid, is obtained as

$$\Omega_d^{st} = \prod_{g\epsilon\{W\}} \Omega_{g,d}^{st} \prod_{l\epsilon L} \Omega_{l,d}^{st} \quad (4)$$

V. Planning Formulation For The Hybrid Microgrid

The proposed formulation is a nonlinear mixed integer problem, according to which the system designer could assign the ac and dc zones and the capacity of the capacitors, rectifiers, inverters, ESS and DG units. For each zone, a set of decision variables are defined: the zone type (ac or dc), sizes of the ESS and different DG units, sizes of the installed rectifiers and inverters in the zone. Furthermore, the sizes of the interlinking converters connection between the neighboring zones are introduced as well. The zone type is defined as a binary variable, takes a value of zero for the dc option or one for the ac option. By considering single-step price curves, which could be simply extended to multistep price curves, the other control variables are continues with values higher than or equal zero.

1. Problem Objective

The objective of this work is to minimize the microgrid total levelized planning cost (5), which comprises the levelized investment and operational costs:

$$\min\ IC + \sum_{d} \mathrm{u_d} \sum_{st} \Omega_d^{st}\ OC_{st,d} \quad (5)$$

The levelized investment cost, the first term in (5), represents the annual investment cost of the DG, ESS and the electronic power converters. More details regarding these items are provided in the following subsection. The second term in (5) represents the levelized operational cost for a year. As stated above, the year is represented by 8 days with different scenarios. The first summation contemplates the occurrence probability of the different scenarios, while the second considers the weight of the day during the year. The constant $\mathrm{u_d}$ for each of the eight days takes a value of 65.22 (365.25/4 day/season × 5/7 weekdays/week) for weekdays and a value of 26.089 (365.25/4 day/season × 2/7 weekends/week) for weekends.

1) The levelized investment cost

It is important to recall that the investment costs are levelized in this analysis to be represented in annual bases for the different microgrid components. The levelized cost is related to the net present value of the total investment cost, which includes capital, installation and maintenance costs, as follows [16]:

$$\begin{aligned} Levelized\ Cost = Total\ invest\ ment\ cost \\ \times CRF\ (i,y) \end{aligned} \quad (6)$$

With

$$CRF\ (i,y) = \frac{i\ (1+i)^y}{(1+i)^y - 1} \quad (7)$$

where CFR is the capital recovery factor and, y is the lifetime of the component, and i is the discount rate.

The type of the zone within the microgrid, i.e., either ac or dc, would impact the components to be installed in this zone, and accordingly alter the investment cost. However, both ac and dc microgrids still have the same basic costs of the ESS and DG components. The levelized investment cost could thus be divided into four items (8-12): the basic installation costs (IC_z'), costs associated with ac zones ($IC_{ac,z}$), costs associated with dc zones ($IC_{dc,z}$), and the interlinking converters cost (IC_t).

$$\begin{aligned} IC = \sum_{z} \left(IC_z' + M_z IC_{ac,z} + (1-M_z)\ IC_{dc,z}\right) \\ + \sum_{t} (M_z - M_{z'})^2\ IC_t \end{aligned} \quad (8)$$

$$IC_z' = \sum_{g\in\{F,W\}} \left(CP_{zg} P_{zg}^{cap}\right) + CP_{zB} P_{Bz}^{cap} + CE_{zB} SoC_{Bz}^{cap} \quad (9)$$

$$IC_{ac,z} = \sum_{g\in\left\{\begin{smallmatrix} F_{dc}, \\ W_{dc},B \end{smallmatrix}\right\}} CI\ P_{zg}^{cap} + \sum_{l\in L_{dc}} CR\ P_{zl}^{max} + CQ\ Q_z^{cap} \quad (10)$$

$$IC_{dc,z} = \sum_{g\in\{F_{ac},W_{ac}\}} CR\ P_{zg}^{cap} + \sum_{z} \sum_{l\in L_{ac}} CIS_{zl}^{max} \quad (11)$$

$$IC_t = \ CT\ S_{t,zz'}^{cap} \quad (12)$$

The basic installation cost comprises the levelized investment cost of the DG and ESS units in different zones, disregarding the zones type (9). It is noteworthy that the ESS levelized investment cost is defined according to its maximum power and maximum SoC. The installation cost of an ac zone ($IC_{ac,z}$) incurs the levelized investment cost of power conversion units (10): inverters to adapt the output power of the ESS and dc-based DG units and rectifiers to feed the dc loads. The costs of the additional capacitors, which provide the system with the VAR required in heavy loading conditions, are included as well in (10). Since $IC_{ac,z}$ is defined only for ac systems, this term is excluded from the total investment cost for dc zones through multiplying $IC_{ac,z}$ by M_z in (8). On contrast, installation of rectifiers and inverters is mandatory for the energy conversion of ac-based DG units and loads, respectively, in dc zones (11). The levelized investment cost of these devices is multiplied by $(1-M_z)$, to exclude the ac zones, and added to the total investment cost (8). Finally, the levelized costs of interlinking converts, between the neighboring zones, are only considered for the ones that connecting ac and dc zones (12).

2) The Daily Operational Cost

For each daily scenario, a twofold operational cost is defined in (13). The first term represents the operational cost of the fuel-based DG units, while as the second incorporates the cost of unserved energy, which reflects the users' willingness to pay in order to avoid power interruptions.

$$\begin{aligned} OC_{st} = \sum_{z} \sum_{h} \sum_{g\epsilon F} CF_g P_{zhg} \\ + \sum_{z} \sum_{h} \sum_{l} \alpha_{zhl}\ \beta_{zhl}^{st}\ P_{zl}^{max}\ CC_{zhl} \end{aligned} \quad (13)$$

2. Problem Constraints

The following constrains must be fulfilled for the solution of each day scenario.

1) The active and reactive power sufficiency constraints:

For each zone, the net summation of DG output powers, ESS injection, and imported active power from the neighboring zones must meet the load after considering the system power loss and spare capacity (14). The spare capacity is introduced to guarantee the microgrid ability in compensating for the sudden and unpredicted increase in its local power demand (i.e., spinning reserve) [17]. For an isolated microgrid, different alternatives can reflect the concept of spare capacity. In this analysis, the spare capacity is represented as specific percentage of the load demand, 5% of the total demand is a reasonable value in isolated microgrids [17]. It is noteworthy that the power loss in the system feeders is also presented as a percentage of the total demand, 5% as well [18].

Similar to the active power constraint, the load reactive power must be supplied via the DG reactive powers, the ESS inverter, the installed capacitors and the imported reactive power form the neighboring zones (15) Since this condition is only applicable in the case of ac zones, the equation is multiplied by the integer variable M_z to relax the condition for dc zones.

$$\sum_{g} P_{hzg}^{net} + \left(P_{hzB}^{dis\_net} - P_{hzB}^{ch\_net}\right) + \sum_{z' \in \eta_z} P_{t,zz'} = \sum_{l} \sigma_z \, \rho_z \, P_{zhL}^{net} \quad \forall h, z \tag{14}$$

$$M_z Q_{hzV} + M_z \sum_{g} Q_{hzg} + M_z Q_{hzB} + M_z \sum_{z' \in \eta_z} Q_{t,zz'} = M_z \sigma_z \, \rho_z Q_{hzl} \quad \forall h, z \tag{15}$$

2) DG Constraints:

The installed DG units must fulfill a set of equality and inequality constraints. It is important to highlight that if the DG type, ac or dc, does not match the zone type, additional conversion loss will be considered. According to [19], the loss of power electronic converts could be represented as a quadratic function in the ac apparent power (16), (17). Thus, Eq. (18) indicates the conversation loss in dc and ac DG units if power converters are required in either ac or dc subgrids

$$F_c(S) = C_2 S^2 + C_1 S + C_0 \tag{16}$$

$${S_{zhg}^{net}}^2 = {P_{zhg}^{net}}^2 + {Q_{zhg}}^2 \quad \forall z, h, g \tag{17}$$

$$P_{zhg}^{loss} = \begin{cases} M_z \, F_c\left(S_{zhg}^{net}\right) & \forall z, h, g \in \{F_{dc}, W_{dc}\} \\ (1 - M_z) F_c\left(P_{zhg}\right) & \forall z, h, g \in \{F_{ac}, W_{ac}\} \end{cases} \tag{18}$$

$$P_{zhg} = P_{zhg}^{loss} + P_{zhg}^{net} \quad \forall z, h, g \tag{19}$$

$$P_{zg}^{min} \leq P_{zhg} \leq P_{zg}^{cap} \quad \forall z, h, g \in \{F\} \tag{21}$$

$$0 \leq P_{zhg} \leq \gamma_{hg}^{st} \, P_{zg}^{cap} \quad \forall z, h, g \in \{W\} \tag{20}$$

$${S_{zhg}}^2 = {P_{zhg}}^2 + M_z {Q_{zhg}}^2 \quad \forall z, h, g \tag{22}$$

$$0 \leq Q_{zhg}, S_{zhg} \leq P_{zg}^{cap} \quad \forall z, h, g \tag{23}$$

3) Capacitors Constraint:

The output reactive power of the capacitors must be less than their installed capacity:

$$0 \leq Q_{hzV} \leq Q_{zhV}^{cap} \quad \forall h, z \tag{24}$$

4) Loads:

The following load constraints count for the load curtailment and the power loss in electronic converters, if implemented. With the consideration of the load curtailment ratio (27), the actual supplied active and reactive powers at the loading terminals are indicated in (25) and (26). Accordingly, the net apparent power is calculated in (28). The active power supplied by the network is obtained in (30) by adding the load power to the power loss associated to the power conversion (29).

$$P_{zhL} = (1 - \alpha_{zhl}) \beta_{zhl}^{st} \, P_{zl}^{max} \quad \forall z, h, l \tag{25}$$

$$Q_{zhL} = (1 - \alpha_{zhl}) \beta_{zhl}^{st} \, Q_{zl}^{max} \quad \forall z, h, l \in \{L_{ac}\} \tag{26}$$

$$0 \leq \alpha_{zhl} \leq 1 \quad \forall z, h, l \tag{27}$$

$${S_{zhl}}^2 = {P_{zhL}}^2 + {Q_{zhl}}^2 \quad \forall z, h, l \in \{L_{ac}\} \tag{28}$$

$$P_{zhL}^{loss} = \begin{cases} M_z \, F_c\left(P_{zhL}^{net}\right) & \forall z, h, l \in \{L_{dc}\} \\ (1 - M_z) F_c\left(S_{zhg}\right) & \forall z, h, l \in \{L_{ac}\} \end{cases} \tag{29}$$

$$P_{zhL}^{net} = P_{zhL} + P_{zhL}^{loss} \quad \forall z, h, l \tag{30}$$

5) ESS Constraints:

The net charging and discharging power of the installed ESS are related via complementary constraint (31) because the ESS could only charge or discharge at any time segment. For ac zones, an additional inverter is installed to adapt the ESS output power to ac. This inverter could support the system reactive power, therefore net apparent power of the ESS is calculated in (32). The inverter loss could be due to either charging or discharging of the ESS in the ac zones only as demonstrated in (33). Relating the ESS power to the net power with the consideration of the inverter loss requires a careful understanding. On other words, the relation between the charging and net charging power is maintained only if the battery is in the charging state (the relationship is bypassed if discharging state is considered). Thus complementary constraints are utilized to handle the problem (34), (35). In (36), the maximum limit of the ESS active, reactive, and apparent powers are maintained. The change in the SoC is calculated as indicated in (37) based on the charging and discharging powers, where the efficiency of charging and discharging cycles is manipulated through η_{ch} and η_{dis} terms. Since optimization problem divides the operation into weighted scenarios during the day, it is a reasonable assumption that the battery is working in a cycle (38) for each scenario to avoid misleading battery operation, i.e., assuming that the battery starts fully charged at the beginning of the day and ends up fully discharged. Finally, the SoC for the ESS must be within a permissible minimum, 30% of the installed capacity is considered in the work, and the ESS maximum SoC capacity (39).

$$0 \leq P_{Bzh}^{ch,net} \perp P_{Bzh}^{dis,net} \geq 0 \quad \forall h, z \tag{31}$$

$${S_{hzB}^{net}}^2 = \left(P_{hzB}^{dis,net} - P_{hzB}^{ch,net}\right)^2 + {Q_{hzB}}^2 \quad \forall h, z \tag{32}$$

$$P_{hzB}^{loss} = M_z\, F_c\left(S_{hzg}^{net}\right) \qquad \forall h,z \qquad (33)$$

$$0 \le P_{Bzh}^{ch} \perp -P_{hzB}^{ch,net} + P_{hzB}^{loss} + P_{hzB}^{ch} \ \ge 0 \qquad \forall h,z \qquad (34)$$

$$0 \le P_{Bzh}^{dis} \perp P_{hzB}^{dis,net} + P_{hzB}^{loss} - P_{hzB}^{dis} \ \ge 0 \qquad \forall h,z \qquad (35)$$

$$0 \le P_{Bzh}^{ch}, P_{Bzh}^{dis}, Q_{hzB}, S_{hzB}^{net}, \le P_{zB}^{cap} \qquad \forall h,z \qquad (36)$$

$$SoC_{Bzh+1} = SoC_{Bzh} + \left(P_{Bzh}^{ch}\eta_{ch} - P_{Bzh}^{dis}/\eta_{dis}\right) \qquad \forall h,z \qquad (37)$$

$$SoC_{Bz,1} = SoC_{Bz,24} + \left(P_{Bz,24}^{ch}\eta_{ch} - P_{Bz,24}^{dis}/\eta_{dis}\right) \qquad \forall z \qquad (38)$$

$$SoC_{zB}^{min} \le SoC_{hzB} \le SoC_{zB}^{cap} \qquad \forall h,z \qquad (39)$$

6) Power Transfer between Neighboring Zones:

It is important to declare that an interlinking converter is assumed between each two neighboring zones. Based on the zones type, this interlinking converter may affect or not the power transfer between the zones. For each zone, the apparent power imported from its neighboring is calculated as illustrated in (40). The power loss in the interlinking converter is represented using (41); the multiplication by the zone type is necessary since the loss is function in the apparent power in the ac side of the converter [19]. In (42), the interlinking converter loss is incorporated to the active power transfer between the neighboring zones if defined with different types; otherwise no power loss is considered. On the other hand, the reactive power transfer between the zones is applicable only if both zones are ac (43). If any of the two-neighboring zone is dc, (43) is relaxed since one of the zones type takes a value of zero. The set of equations in (44-46) governs the maximum active, reactive and apparent power that a zone could exchange with its neighbor through an interlinking converter. These set of equations are not applied, i.e. relaxed, for neighboring zones with similar types.

$$S_{ht,zz'}{}^2 = P_{ht,zz'}{}^2 + Q_{ht,zz'}{}^2 \qquad \forall h,t \qquad (40)$$

$$P_{ht,zz'}^{loss} = M_z\, F_c\left(S_{ht,zz'}\right) + M_{z'}F_c\left(S_{ht,z'z}\right) \qquad \forall h,t \qquad (41)$$

$$P_{ht,zz'} + P_{ht,z'z} + (M_z - M_{z'})^2 P_{ht,zz'}^{loss} = 0 \qquad \forall h,t \qquad (42)$$

$$\left(Q_{t,z'z} + Q_{t,zz'}\right)M_z M_{z'} = 0 \qquad \forall h,t \qquad (43)$$

$$-S_{t,zz'}^{cap} \le (M_z - M_{z'})^2 P_{ht,zz'} \le S_{t,zz'}^{cap} \qquad \forall h,t \qquad (44)$$

$$-S_{t,zz'}^{cap} \le (M_z - M_{z'})^2 Q_{ht,zz'} \le S_{t,zz'}^{cap} \qquad \forall h,t \qquad (45)$$

$$0 \le (M_z - M_{z'})^2\, S_{ht,zz'} \le S_{t,zz'}^{cap} \qquad \forall h,t \qquad (46)$$

VI. Case Studies

The inputs and outputs for the developed planning model are summarized as follows:

1. Inputs:

- Number of neighbor zones with predefined possible interconnections.
- The ac and dc load profiles inside each zone.
- Historical data for the renewable energy resources which depend on zone's location.
- Different costs associated with renewable-based DGs, energy storage units, dispatchable DGs, capacitors and load curtailment.

2. Outputs:

- The type of each zone either ac or dc.
- The size of the interlinking converter if needed.
- The DER mix for each zone. This means setting sizes for renewable DGs, dispatchable DGs, energy storage units, and capacitors.
- The minimum levelized planning cost.

TABLE I: Levelized costs for different types of generation

Generation type	Capital $/MWh	Fixed O&M $/MWh	Variable O&M $/MWh
Wind	42.1	13.4	NA
Solar	66.9	9.9	NA
ac dispatchable	12.3	1.4	35.2
dc dispatchable	36.3	6.5	50.2

To validate the proposed planning model, an illustrative system with the layout shown in Fig. 1 is considered. This system has three zones with two interconnection ties between zones {1,2} and {2,3}. To study the effectiveness of the proposed planning model, three different planning scenarios for this system are investigated as follows:

- Scenario a: the optimal configuration is examined with no constraints imposed on the type of zones or generation units.
- Scenario b: all zones are assumed to have the same type either ac or dc with unconstrained generation type.
- Scenario c: all zones are assumed to have the same type with constrained generation type to be same as zone type.
- Scenario d: extension zone is assumed to take place while two zones already exist.

For all scenarios, the historical data for wind speed and solar irradiance presented in [20] and their corresponding output power PDFs are adopted in this study. As described in section IV, the PDFs are discretized to obtain the normalized power states for renewable-based DGs in all zones. In addition, for each zone a combination of residential, commercial and industrial load profiles presented in [21] is assumed to represent the ac and dc load profiles in this zone. The capital and O&M costs for different generation types as presented in TABLE I are used for units allocated in any zone.

1. Scenario a

The optimal configuration of the system obtained for this scenario is $M_z = \{0,\ 1,\ 1\}$. This configuration resulted in the minimum levelized planning cost as presented in Table II. Therefore, the optimal configuration of the system is: zone 1 dc-zone with an interlinking converter connection to zone 2 while the other two zones are ac-zones and thus connected with a direct link. Fig. 4 presents the obtained optimal DER mix in each zone that satisfies the system constraints with the minimum levelized planning cost. Although zone 1 is a dc-zone, the obtained DER mix is not solely dc and similarly

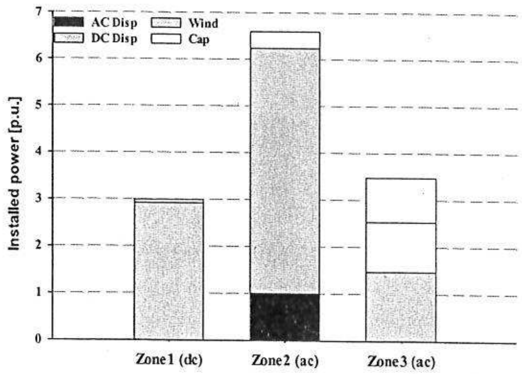

Fig. 4. Optimal energy resource mix for scenario a

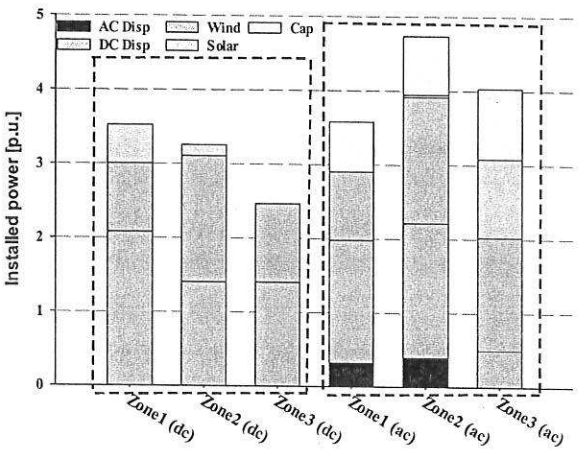

Fig. 5. Optimal energy resource mix for scenario b

zones 2 and 3 are ac-zones with a dc-generation selected in their optimal DER mix. This proves the significant effect of load and renewable generation probabilistic characteristics on the planning decisions. Therefore, selecting the type of generation to match the type of zone is not an optimal approach.

2. Scenario b

All zones are constrained to have the same type either ac or dc. This scenario was examined using the presented planning model through adding a constraint $M_z = \{1, 1, 1\}$ or $M_z = \{0, 0, 0\}$, respectively. Accordingly, the planning framework set the optimal DER mix that has the minimum feasible levelized planning cost while satisfies all system's constraints as explained in section V. The optimal DER mix obtained for this scenario is shown in Fig. 5 and the associated levelized planning costs are compared to the optimal system configuration case (scenario a) as presented in TABLE II.

The obtained results demonstrate the effect of considering the system type as a planning decision-variable on curtailing the levelized planning cost significantly. Furthermore, the constrained planning scenarios comprise lower renewable capacities compared to the unconstrained scenario. Evident by the results obtained, the optimal DER mix for a defined system configuration is challenging and depends on the probabilistic nature of load and generation as well as the capital and O&M costs.

3. Scenario c

All zones are constrained to be dc and all DGs are constrained to match the zone type. This scenario was examined using the presented planning model through adding a constraint $M_z = \{0, 0, 0\}$ and setting the maximum capacity constraints for wind-based, capacitor units and ac-dispatchable DGs to zero. The optimal DER mix obtained for this case is shown in Fig. 6. The selected mix has solar-based DGs, and dc-dispatchable DGs to satisfy power sufficiency and transfer constraints. As presented in TABLE VII, the levelized planning cost for this scenario is almost elevated by 7.75% compared to the optimal configuration case for the {0,0,0} system, while supplying the same load. These findings highlight that as the planning problem gets more constrained, the levelized planning cost increases for the same system load. Thus, modeling of the problem with flexible planning decisions as presented in this framework is crucial to achieve the minimal levelized planning cost.

4. Scenario d

In contrary to the previous scenarios which consider planning of newly constructed zones, this scenario studies extending an existing system by constructing a new zone. Consequently, the DER mix for the existing system is defined and invariant. To examine this scenario, the system shown in Fig. 1 is considered with zones 2 and 3 assumed to be of ac type. The DER mix for each of the two zones was adopted from the results obtained for scenario b. System constraints in the proposed model was modified to reflect these predefined sizing conditions in addition to constraining zone types with $M_z = 1\ \forall z \in \{2,3\}$. Zone 1 was assumed to be the extension of this existing system and the proposed framework is employed for this planning scenario. The optimal DER mix obtained for zone 1 in this case is shown in Fig. 7 and the optimal type of zone 1 was found to be dc. The minimum levelized planning cost achieved in this scenario was 1.2317M$ which represents almost 10 % savings compared to all ac configuration.

VII. CONCLUSION

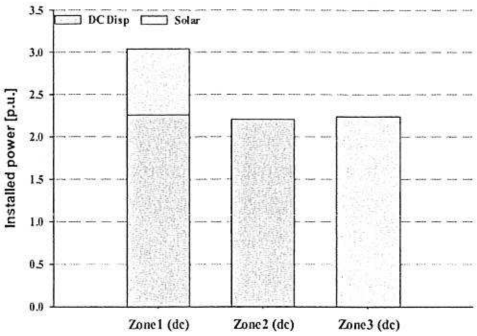

Fig. 6. Optimal ac energy resource mix for scenario c

TABLE II LEVELIZED PLANNING COST FOR DIFFERENT SYSTEM CONFIGURATIONS

Scenario a {0,1,1}	Scenario b	Scenario c {0,0,0}
1.1514 M$	{0,0,0}: 1.2688M$ {1,1,1}:1.3503M$	1.367M$

This paper presented a planning framework for hybrid ac-dc microgrids. The planning model was designed to consider the probabilistic nature of renewable-based generation and loads. The problem was formulated as a MINLP that minimizes the levelized planning cost subjected to system's and components' constraints. All components' practical constraints were contemplated in the model such as DG's constraints, battery energy storage constraints, capacitor constraints, etc. Moreover, the levelized planning cost considered both investment and O&M costs. The control variables used in the model were the DER mix, the type of microgrid, and the size of deployed interlinking converters. In this regard, the optimal DER mix included the size of renewable-based DGs, dispatchable DGs, energy storage, and capacitors.

In order to proof the effectiveness and flexibility of the framework, several case studies and planning scenarios were investigated. These scenarios demonstrated the capability of applying the proposed framework for planning newly constructed system or extending an existing system by adding a microgrid. The obtained results indicated the potency of the developed model in obtaining the optimal system configuration given the randomness of load and renewables. The case studies showed a significant reduction in the levelized planning cost when the type of the microgrid was considered as a decision variable.

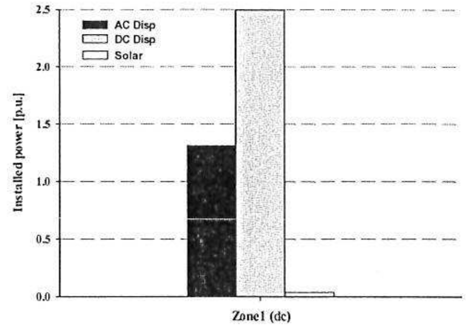

Fig. 7. Optimal energy resources mix for zone 3 as an extension

REFERENCES

[1] E. Jung, H. Yoo, S.-K. Sul, H.-S. Choi, and Y.-Y. Choi, "A Nine-Phase Permanent-Magnet Motor Drive System for an Ultrahigh-Speed Elevator," *IEEE Trans. Ind. Appl.*, vol. 48, no. 3, pp. 987–995, May 2012.

[2] G. Reed, B. Grainger, A. Sparacino, and Z.-H. Mao, "Ship to Grid: Medium-Voltage DC Concepts in Theory and Practice," *IEEE Power Energy Mag.*, vol. 10, no. 6, pp. 70–79, Nov. 2012.

[3] A. A. Hamad, M. A. Azzouz, and E. F. El Saadany, "A Sequential Power Flow Algorithm for Islanded Hybrid AC/DC Microgrids," *IEEE Trans. Power Syst.*, vol. PP, no. 99, pp. 1–10, 2015.

[4] A. Mohamed, V. Salehi, and O. Mohammed, "Real-Time Energy Management Algorithm for Mitigation of Pulse Loads in Hybrid Microgrids," *IEEE Trans. Smart Grid*, vol. 3, no. 4, pp. 1911–1922, Dec. 2012.

[5] S. A. Arefifar and Y. A.-R. I. Mohamed, "Probabilistic Optimal Reactive Power Planning in Distribution Systems With Renewable Resources in Grid-Connected and Islanded Modes," *IEEE Trans. Ind. Electron.*, vol. 61, no. 11, pp. 5830–5839, Nov. 2014.

[6] J. Xiao, L. Bai, F. Li, H. Liang, and C. Wang, "Sizing of Energy Storage and Diesel Generators in an Isolated Microgrid Using Discrete Fourier Transform (DFT)," *IEEE Trans. Sustain. Energy*, vol. 5, no. 3, pp. 907–916, Jul. 2014.

[7] G. Diaz, C. Gonzalez-Moran, J. Gomez-Aleixandre, and A. Diez, "Scheduling of Droop Coefficients for Frequency and Voltage Regulation in Isolated Microgrids," *IEEE Trans. Power Syst.*, vol. 25, no. 1, pp. 489–496, Feb. 2010.

[8] M. M. A. Abdelaziz and E. F. El-Saadany, "Maximum loadability consideration in droop-controlled islanded microgrids optimal power flow," *Electr. Power Syst. Res.*, vol. 106, pp. 168–179, 2014.

[9] M. M. A. Abdelaziz, H. E. Farag, and E. F. El-Saadany, "Optimum Droop Parameter Settings of Islanded Microgrids With Renewable Energy Resources," *IEEE Trans. Sustain. Energy*, vol. PP, no. 99, pp. 1–1, Apr. 2014.

[10] H. Lotfi and A. Khodaei, "AC Versus DC Microgrid Planning," *IEEE Trans. Smart Grid*, vol. PP, no. 99, pp. 1–1, 2015.

[11] H. M. A. Ahmed, A. B. Eltantawy, and M. M. A. Salama, "A Planning Approach for the Network Configuration of AC-DC Hybrid Distribution Systems," *IEEE Trans. Smart Grid*, pp. 1–1, 2016.

[12] S. Mashayekh and K. L. Butler-Purry, "An Integrated Security-Constrained Model-Based Dynamic Power Management Approach for Isolated Microgrids in All-Electric Ships," *IEEE Trans. Power Syst.*, vol. 30, no. 6, pp. 2934–2945, Nov. 2015.

[13] Z. Zhao, P. Yang, J. Guerrero, Z. Xu, and T. Green, "Multiple-Time-Scales Hierarchical Frequency Stability Control Strategy of Medium-Voltage Isolated Microgrid," *IEEE Trans. Power Electron.*, vol. 31, no. 8, pp. 1–1, 2015.

[14] M. E. Nassar and M. M. A. Salama, "Adaptive Self-Adequate Microgrids Using Dynamic Boundaries," *IEEE Trans. Smart Grid*, vol. 7, no. 1, pp. 105–113, Jan. 2016.

[15] Y. M. Atwa, E. F. El-Saadany, M. M. A. Salama, R. Seethapathy, M. Assam, and S. Conti, "Adequacy Evaluation of Distribution System Including Wind/Solar DG During Different Modes of Operation," *IEEE Trans. Power Syst.*, vol. 26, no. 4, pp. 1945–1952, Nov. 2011.

[16] W. G. Willis, H. L., & Scott, *Distributed Power Generation: Planning and Evaluation*. New York: CRC Press, 2000.

[17] C. A. Hernandez-Aramburo, T. C. Green, and N. Mugniot, "Fuel Consumption Minimization of a Microgrid," *IEEE Trans. Ind. Appl.*, vol. 41, no. 3, pp. 673–681, May 2005.

[18] Y. M. Atwa, E. F. El-Saadany, M. M. A. Salama, R. Seethapathy, M. Assam, and S. Conti, "Adequacy Evaluation of Distribution System Including Wind/Solar DG During Different Modes of Operation," *IEEE Trans. Power Syst.*, vol. 26, no. 4, pp. 1945–1952, Nov. 2011.

[19] J. Beerten, S. Cole, and R. Belmans, "Generalized Steady-State VSC MTDC Model for Sequential AC/DC Power Flow Algorithms," *IEEE Trans. Power Syst.*, vol. 27, no. 2, pp. 821–829, May 2012.

[20] H. E. Z. Farag and E. F. El-Saadany, "A Novel Cooperative Protocol for Distributed Voltage Control in Active Distribution Systems," *IEEE Trans. Power Syst.*, vol. 28, no. 2, pp. 1–1, May 2013.

[21] J. A. Jardini, C. M. V. Tahan, M. R. Gouvea, S. U. Ahn, and F. M. Figueiredo, "Daily load profiles for residential, commercial and industrial low voltage consumers," *IEEE Trans. Power Deliv.*, vol. 15, no. 1, pp. 375–380, 2000.